Fractal Structures in Condensed Matter Physics

TSUNEYOSHI NAKAYAMA
Toyota Physical and Chemical Research Institute, Nagakute, Japan

Article Outline

Glossary
Definition of the Subject
Introduction
Determining Fractal Dimensions
Polymer Chains in Solvents
Aggregates and Flocs
Aerogels
Dynamical Properties of Fractal Structures
Spectral Density of States and Spectral Dimensions
Future Directions
Bibliography

Glossary

Anomalous diffusion It is well known that the mean-square displacement $\langle r^2(t)\rangle$ of a diffusing particle on a uniform system is proportional to the time t such

as $\langle r^2(t)\rangle \sim t$. This is called *normal diffusion*. Particles on fractal networks diffuse more slowly compared with the case of normal diffusion. This slow diffusion called *anomalous diffusion* follows the relation given by $\langle r^2(t)\rangle \sim t^a$, where the condition $0 < a < 1$ always holds.

Brownian motion Einstein published the important paper in 1905 opening the way to investigate the movement of small particles suspended in a stationary liquid, the so-called Brownian motion, which stimulated J. Perrin in 1909 to pursue his experimental work confirming the atomic nature of matter. The trail of a random walker provides an instructive example for understanding the meaning of random fractal structures.

Fractons Fractons, excitations on fractal elastic-networks, were named by S. Alexander and R. Orbach in 1982. Fractons manifest not only static properties of fractal structures but also their dynamic properties. These modes show unique characteristics such as strongly localized nature with the localization length of the order of wavelength.

Spectral density of states The spectral density of states of ordinary elastic networks are expressed by the Debye spectral density of states given by $D(\omega) \sim \omega^{d-1}$, where d is the Euclidean dimensionality. The spectral density of states of fractal networks is given by $D(\omega) \sim \omega^{d_s-1}$, where d_s is called the spectral or fracton dimension of the system.

Spectral dimension This exponent characterizes the spectral density of states for vibrational modes excited on fractal networks. The spectral dimension constitutes the dynamic exponent of fractal networks together with the conductivity exponent and the exponent of anomalous diffusion.

Definition of the Subject

The idea of fractals is based on *self-similarity*, which is a symmetry property of a system characterized by invariance under an isotropic scale-transformation on certain length scales. The term *scale-invariance* has the implication that objects look the same on different scales of observations. While the underlying concept of fractals is quite simple, the concept is used for an extremely broad range of topics, providing a simple description of highly complex structures found in nature. The term *fractal* was first introduced by Benoit B. Mandelbrot in 1975, who gave a definition on fractals in a simple manner "*A fractal is a shape made of parts similar to the whole in some way*". Thus far, the concept of fractals has been extensively used to understand the behaviors of many complex systems or has been applied from physics, chemistry, and biology for applied sciences and technological purposes. Examples of fractal structures in condensed matter physics are numerous such as polymers, colloidal aggregations, porous media, rough surfaces, crystal growth, spin configurations of diluted magnets, and others. The critical phenomena of phase transitions are another example where self-similarity plays a crucial role. Several books have been published on fractals and reviews concerned with special topics on fractals have appeared.

Length, area, and volume are special cases of ordinary Euclidean *measures*. For example, length is the measure of a one-dimensional (1d) object, area the measure of a two-dimensional (2d) object, and volume the measure of a three-dimensional (3d) object. Let us employ a physical quantity (observable) as the measure to define dimensions for Euclidean systems, for example, a total mass $M(r)$ of a fractal object of the size r. For this, the following relation should hold

$$r \propto M(r)^{1/d} , \tag{1}$$

where d is the Euclidean dimensionality. Note that Euclidean spaces are the simplest scale-invariant systems. We extend this idea to introduce dimensions for self-similar fractal structures. Consider a set of particles with unit mass m randomly distributed on a d-dimensional Euclidean space called the *embedding space* of the system. Draw a sphere of radius r and denote the total mass of particles included in the sphere by $M(r)$. Provided that the following relation holds *in the meaning of statistical average* such as

$$r \propto \langle M(r)\rangle^{1/D_f} , \tag{2}$$

where $\langle \ldots \rangle$ denotes the ensemble-average over different spheres of radius r, we call D_f the *similarity dimension*. It is necessary, of course, that D_f is smaller than the embedding Euclidean dimension d. The definition of dimension as a *statistical quantity* is quite useful to specify the characteristic of a self-similar object if we could choose a suitable measure.

There are many definitions to allocate dimensions. Sometimes these take the same value as each other and sometimes not. The *capacity dimension* is based on the coverage procedure. As an example, the length of a curved line L is given by the product of the number N of straight-line segment of length r needed to step along the curve from one end to the other such as $L(r) = N(r)r$. While, the area $S(r)$ or the volume $V(r)$ of arbitrary objects can be measured by covering it with squares or cubes of linear

size r. The identical relation,

$$M(r) \propto N(r) r^d \tag{3}$$

should hold for the total mass $M(r)$ as measure, for example. If this relation does not change as $r \to 0$, we have the relation $N(r) \propto r^{-d}$. We can extend the idea to define the dimensions of fractal structures such as

$$N(r) \propto r^{-D_\mathrm{f}} , \tag{4}$$

from which the *capacity dimension* D_f is given by

$$D_\mathrm{f} := \lim_{r \to 0} \frac{\ln N(r)}{\ln(1/r)} . \tag{5}$$

The definition of D_f can be rendered in the following implicit form

$$\lim_{r \to 0} N(r) r^{D_\mathrm{f}} = \text{const} . \tag{6}$$

Equation (5) brings out a key property of the *Hausdorff dimension* [10], where the product $N(r)r^{D_\mathrm{f}}$ remains finite as $r \to 0$. If D_f is altered even by an infinitesimal amount, this product will diverge either to zero or to infinity. The Hausdorff dimension coincides with the capacity dimension for many fractal structures, although the Hausdorff dimension is defined less than or equal to the capacity dimension. Hereafter, we refer to the capacity dimension or the Hausdorff dimension mentioned above as the *fractal dimension*.

Introduction

Fractal structures are classified into two categories; *deterministic* fractals and *random* fractals. In condensed matter physics, we encounter many examples of random fractals. The most important characteristic of random fractals is the spatial and/or sample-to-sample fluctuations in their properties. We must discuss their characteristics by averaging over a large ensemble. The nature of deterministic fractals can be easily understood from some examples. An instructive example is the *Mandelbrot–Given fractal* [12], which can be constructed by starting with a structure with eight line segments as shown in Fig. 1a (the first stage of the Mandelbrot–Given fractal). In the second stage, each line segment of the initial structure is replaced by the initial structure itself (Fig. 1b). This process is repeated indefinitely. The Mandelbrot–Given fractal possesses an obvious dilatational symmetry, as seen from Fig. 1c, i. e., when we magnify a part of the structure, the enlarged portion looks just like the original one. Let us apply (5) to determine D_f of the Mandelbrot–Given fractal. The Mandelbrot–Given fractal is composed of 8 parts of size 1/3, hence, $N(1/3) = 8$, $N((1/3)^2) = 8^2$, and so on. We thus have a relation of the form $N(r) \propto r^{-\ln_3 8}$, which gives the fractal dimension $D_\mathrm{f} = \ln_3 8 = 1.89278\ldots$. The Mandelbrot–Given fractal has many analogous features with *percolation networks* (see Sect. "Dynamical Properties of Fractal Structures"), a typical random fractal, such that the fractal dimension of a 2d percolation network is $D_\mathrm{f} = 91/48 = 1.895833\ldots$, which is very close to that of the Mandelbrot–Given fractal.

The geometric characteristics of random fractals can be understood by considering two extreme cases of random structures. Figure 2a represents the case in which particles are randomly but *homogeneously* distributed in a d-dimensional box of size L, where d represents ordinary Euclidean dimensionality of the embedding space. If we divide this box into smaller boxes of size l, the *mass density* of the ith box is

$$\rho_i(l) = \frac{M_i(l)}{l^d} , \tag{7}$$

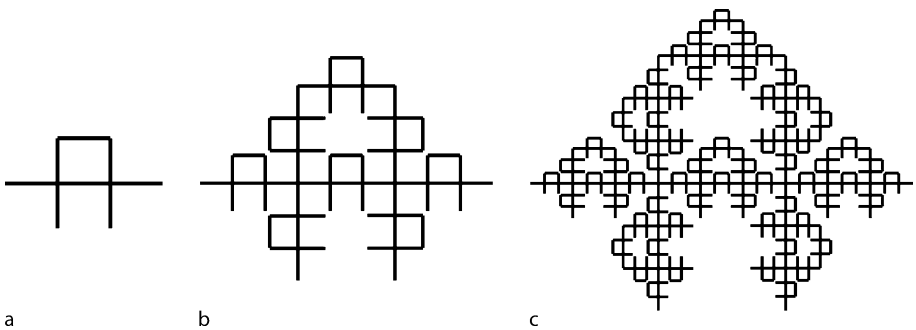

Fractal Structures in Condensed Matter Physics, Figure 1
Mandelbrot–Given fractal. a The initial structure with eight line segments, b the object obtained by replacing each line segment of the initial structure by the initial structure itself (the second stage), and c the third stage of the Mandelbrot–Given fractal obtained by replacing each line segment of the second-sage structure by the initial structure

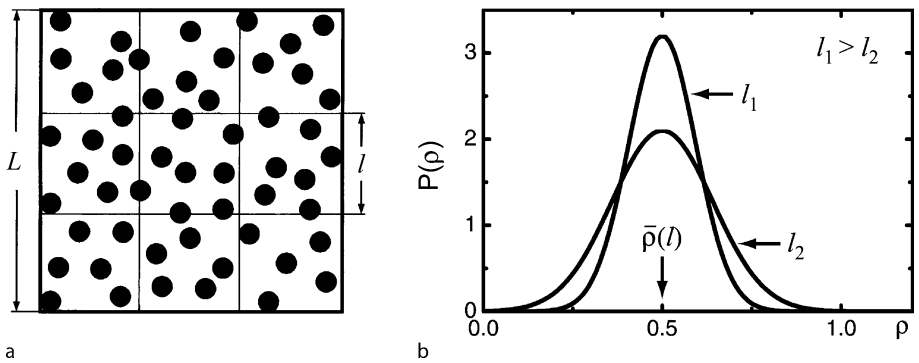

Fractal Structures in Condensed Matter Physics, Figure 2
a Homogeneous random structure in which particles are randomly but homogeneously distributed, and b the distribution functions of local densities ρ, where $\overline{\rho}(l)$ is the average mass density independent of l

where $M_i(l)$ represents the total mass (measure) inside box i. Since this quantity depends on the box i, we plot the distribution function $P(\rho)$, from which curves like those in Fig. 2b may be obtained for two box sizes l_1 and $(l_2 < l_2)$. We see that the central peak position of the distribution function $P(\rho)$ is the same for each case. This means that the average mass density yields

$$\overline{\rho}(l) = \frac{\langle M_i(l)\rangle_i}{l^d}$$

becomes constant, indicating that $\langle M_i(l)\rangle_i \propto l^d$. The above is equivalent to

$$\overline{\rho} = \frac{m}{\overline{a}^d}\,, \tag{8}$$

where $\overline{a}$ is the average distance (characteristic length-scale) between particles and the mass of a single particle. This indicates that there exists a single length scale $\overline{a}$ characterizing the random system given in Fig. 2a.

The other type of random structure is shown in Fig. 3a, where particle positions are correlated with each other and $\rho_i(l)$ greatly fluctuates from box to box, as shown in Fig. 3b. The relation $\langle M_i(l)\rangle_i \propto l^d$ may not hold at all for this type of structure. Assuming the fractality for this system, namely, if the power law $\langle M_i(l)\rangle_i \propto l_{\rm f}^D$ holds, the average mass density becomes

$$\bar{\rho}(l) = \frac{\langle M_i(l)\rangle_i}{l^d} \propto l^{D_{\rm f}-d}\,, \tag{9}$$

where $\rho_i(l) = 0$ is excluded. In the case $D_{\rm f} < d$, $\bar{\rho}(l)$ depends on l and decreases with increasing l. Thus, there is no characteristic length scale for the type of random structure shown in Fig. 3a. If (9) holds with $D_{\rm f} < d$, so that $\langle M_i(l)\rangle_i$ is proportional to $l_{\rm f}^D$, the structure is said to be *fractal*. It is important to note that there is no *characteristic length scale* for the type of random fractal structure shown in Fig. 3b. Thus, we can extend the idea of self-similarity not only for deterministic self-similar structures, but also

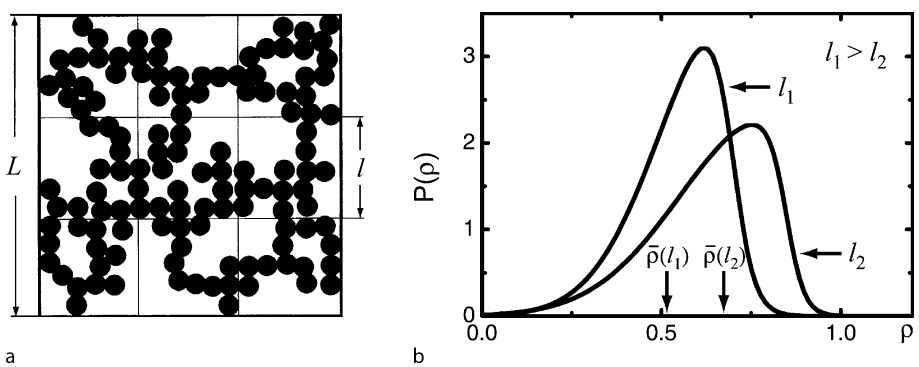

Fractal Structures in Condensed Matter Physics, Figure 3
a Correlated random fractal structure in which particles are randomly distributed, but correlated with each other, and b the distribution functions of local densities ρ with finite values, where the average mass densities depend on l

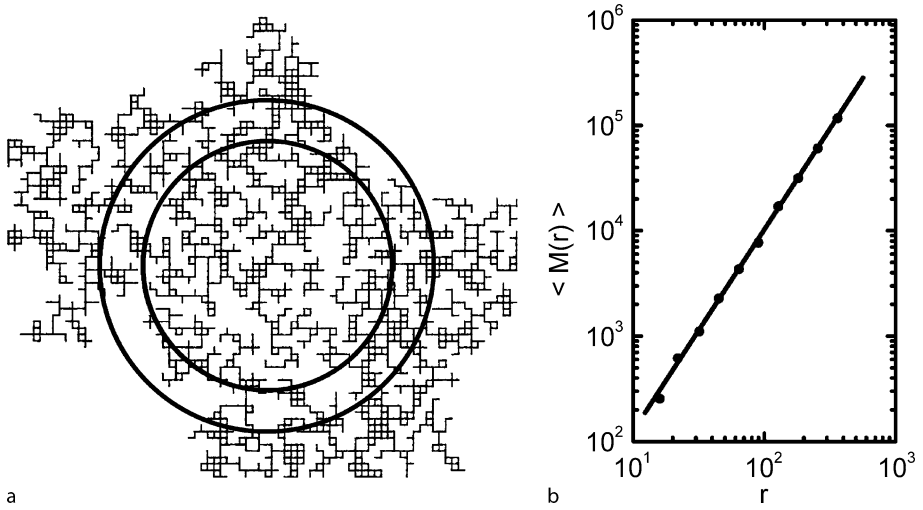

Fractal Structures in Condensed Matter Physics, Figure 4
a 2d site-percolation network and circles with different radii. b The power law relation holds between *r* and the number of particles in the sphere of radius *r*, indicating the fractal dimension of the 2d network is $D_f = 1.89\ldots = 91/48$

for random and disordered structures, the so-called *random fractals*, in the meaning of statistical average.

The percolation network made by putting particles or bonds on a lattice with the probability p is a typical example of random fractals. The theory of percolation was initiated in 1957 by S.R. Broadbent and J.M. Hammersley [5] in connection with the diffusion of gases through porous media. Since their work, it has been widely accepted that the percolation theory describes a large number of physical and chemical phenomena such as gelation processes, transport in amorphous materials, hopping conduction in doped semiconductors, the quantum Hall effect, and many other applications. In addition, it forms the basis for studies of the flow of liquids or gases through porous media. Percolating networks thus serve as a model which helps us to understand physical properties of complex fractal structures.

For both deterministic and random fractals, it is remarkable that no characteristic length scale exists, and this is a key feature of fractal structures. In other words, fractals are defined to be objects invariant under isotropic scale transformations, i. e., uniform dilatation of the system in every spatial direction. In contrast, there exist systems which are invariant under *anisotropic* transformations. These are called *self-affine fractals*.

Determining Fractal Dimensions

There are several methods to determine fractal dimensions D_f of complex structures encountered in condensed matter physics. The following methods for obtaining the fractal dimension D_f are known to be quite efficient.

Coverage Method

The idea of coverage in the definition of the capacity dimension (see (5)) can be applied to obtain the fractal dimension D_f of material surfaces. An example is the fractality of rough surfaces or inner surfaces of porous media. The fractal nature is probed by changing the sizes of adsorbed molecules on solid surfaces. Power laws are verified by plotting the total number of adsorbed molecules versus their size r. The area of a surface can be estimated with the aid of molecules weakly adsorbed by van der Waals forces. Gas molecules are adsorbed on empty sites until the surface is uniformly covered with a layer one molecule thick. Provided that the radius r of one adsorbed molecule and the number of adsorbed molecules $N(r)$ are known, the surface area S obtained by molecules is given by

$$S(r) \propto N(r) r^2 \,. \tag{10}$$

If the surface of the adsorbate is perfectly smooth, we expect the measured area to be independent of the radius r of the probe molecules, which indicates the power law

$$N(r) \propto r^{-2} \,. \tag{11}$$

However, if the surface of the adsorbate is rough or contains pores that are small compared with r, less of the surface area S is accessible with increasing size r. For a fractal

surface with fractal dimension D_f, (11) gives the relation

$$N(r) \propto r^{-D_f} . \tag{12}$$

Box-Counting Method

Consider as an example a set of particles distributed in a space. First, we divide the space into small boxes of size r and count the number of boxes containing more than one particle, which we denote by $N(r)$. From the definition of the capacity dimension (4), the number of particle

$$N(r) \propto r^{-D_f} . \tag{13}$$

For homogeneous objects distributed in a d-dimensional space, the number of boxes of size r becomes, of course

$$N(r) \propto r^{-d} .$$

Correlation Function

The fractal dimension D_f can be obtained via the correlation function, which is the fundamental statistical quantity observed by means of X-ray, light, and neutron scattering experiments. These techniques are available to bulk materials (not surface), and is widely used in condensed matter physics. Let $\rho(\boldsymbol{r})$ be the number density of atoms at position $\boldsymbol{r}$. The density-density correlation function $G(\boldsymbol{r}, \boldsymbol{r}')$ is defined by

$$G(\boldsymbol{r}, \boldsymbol{r}') = \langle \rho(\boldsymbol{r})\rho(\boldsymbol{r}') \rangle , \tag{14}$$

where $\langle \ldots \rangle$ denotes an ensemble average. This gives the correlation of the number-density fluctuation. Provided that the distribution is isotropic, the correlation function becomes a function of only one variable, the radial distance $r = |\boldsymbol{r} - \boldsymbol{r}'|$, which is defined in spherical coordinates. Because of the translational invariance of the system on average, $\boldsymbol{r}'$ can be fixed at the coordinate origin $\boldsymbol{r}' = 0$. We can write the correlation function as

$$G(\boldsymbol{r}) = \langle \rho(\boldsymbol{r})\rho(0) \rangle . \tag{15}$$

The quantity $\langle \rho(\boldsymbol{r})\rho(0) \rangle$ is proportional to the probability that a particle exists at a distance r from another particle. This probability is proportional to the particle density $\rho(r)$ within a sphere of radius r. Since $\rho(r) \propto r^{D_f - d}$ for a fractal distribution, the correlation function becomes

$$G(\boldsymbol{r}) \propto r^{D_f - d} , \tag{16}$$

where D_f and d are the fractal and the embedded Euclidean dimensions, respectively. This relation is often used directly to determine D_f for random fractal structures.

The scattering intensity in an actual experiment is proportional to the structure factor $S(q)$, which is the Fourier transform of the correlation function $G(r)$. The structure factor is calculated from (16) as

$$S(q) = \frac{1}{V} \int_V G(r) \mathrm{e}^{iq \cdot r} \mathrm{d}r \propto q^{-D_f} \tag{17}$$

where V is the volume of the system. Here $\mathrm{d}r$ is the d-dimensional volume element. Using this relation, we can determine the fractal dimension D_f from the data obtained by scattering experiments.

When applying these methods to obtain the fractal dimension D_f, we need to take care over the following point. Any fractal structures found in nature must have upper and lower length-limits for their fractality. There usually exists a *crossover* from homogeneous to fractal. Fractal properties should be observed only between these limits.

We describe in the succeeding Sections several examples of fractal structures encountered in condensed matter physics.

Polymer Chains in Solvents

Since the concept of fractal was coined by B.B. Mandelbrot in 1975, scientists reinterpreted random complex structures found in condensed matter physics in terms of fractals. They found that a lot of objects are classified as fractal structures. We show at first from polymer physics an instructive example exhibiting the fractal structure. That is an early work by P.J. Flory in 1949 on the relationship between the mean-square end-to-end distance of a polymer chain $\langle r^2 \rangle$ and the degree of polymerization N. Consider a dilute solution of separate coils in a solvent, where the total length of a flexible polymer chain with a monomer length a is Na. The simplest idealization views the polymer chain in analogy with a *Brownian motion* of a random walker. The walk is made by a succession of N steps from the origin $\boldsymbol{r} = 0$ to the end point $\boldsymbol{r}$. According to the *central limit theorem* of the probability theory, the probability to find a walker at $\boldsymbol{r}$ after N steps ($N \gg 1$) follows the *diffusion equation* and we have the expression for the probability to find a particle after N steps at $\boldsymbol{r}$

$$P_N(\boldsymbol{r}) = (2\pi N a^2/3)^{-3/2} \exp(-3r^2/2Na^2) , \tag{18}$$

where the prefactor arises from the normalization of $P_N(\boldsymbol{r})$. The mean squared distance calculated from $P_N(\boldsymbol{r})$ becomes

$$\langle \boldsymbol{r}^2 \rangle = \int r^2 P_N(\boldsymbol{r}) \mathrm{d}^3\boldsymbol{r} = Na^2 . \tag{19}$$

Then, the mean-average end-to-end distance of a polymer chain yields $R = \langle r^2 \rangle^{1/2} = N^{1/2}a$. Since the number

of polymerization N corresponds to the total mass M of a polymer chain, the use of (19) leads to the relation such as $M(R) \sim R^2$. The mass $M(R)$ can be considered as a measure of a polymer chain, the fractal dimension of this ideal chain as well as the trace of Brown motion becomes $D_f = 2$ for any d-dimensional embedding space.

The entropy of the idealized chain of the length $L = Na$ is obtained from (18) as

$$S(r) = S(0) - \frac{3r^2}{2R^2} , \tag{20}$$

from which the free energy $F_{el} = U - TS$ is obtained as

$$F_{el}(r) = F_{el}(0) + \frac{3k_B Tr^2}{2R^2} . \tag{21}$$

Here U is assumed to be independent of distinct configurations of polymer chains. This is an elastic energy of an ideal chain due to entropy where F_{el} decreases as $N \to$ large. P.J. Flory added the repulsive energy term due to monomer-monomer interactions, the so-called *excluded volume effect*. This has an analogy with *self-avoiding random walk*. The contribution to the free energy is obtained by the virial expansion into the power series on the concentration $c_{int} = N/r^d$. According to the mean field theory on the repulsive term $F_{int} \propto c_{int}^2$, we have the total free-energy F such as

$$\frac{F}{k_B T} = \frac{3r^2}{2Na^2} + \frac{v(T)N^2}{r^d} , \tag{22}$$

where $v(T)$ is the excluded volume parameter. We can obtain a minimum of $F(r)$ at $r = R$ by differentiating $F(r)$ with respect to r such that

$$M(R) \propto R^{\frac{d+2}{3}} . \tag{23}$$

Here the number of polymerization N corresponds to the total mass $M(R)$ of a polymer chain. Thus, we have the fractal dimension $D_f = (d + 2)/3$, in particular, $D_f = 5/3 = 1.666\ldots$ for a polymer chain in a solvent.

Aggregates and Flocs

The structures of a wide variety of flocculated colloids in suspension (called aggregates or flocs) can be described in terms of *fractals*. A colloidal suspension is a fluid containing small charged particles that are kept apart by Coulomb repulsion and kept afloat by Brownian motion. A change in the particle-particle interaction can be induced by varying the chemical composition of the solution and in this manner an aggregation process can be initiated. Aggregation processes are classified into two simple types: diffusion-limited aggregation (DLA) and diffusion-limited cluster-cluster aggregation (DLCA), where a DLA is due to the cluster-particle coalescence and a DLCA to the cluster-cluster flocculation. In most cases, actual aggregates involve a complex interplay between a variety of flocculation processes. The pioneering work was done by M.V. Smoluchowski in 1906, who formulated a kinetic theory for the irreversible aggregation of particles into clusters and further clusters combining with clusters. The inclusion of cluster-cluster aggregation makes this process distinct from the DLA process due to particle-cluster interaction. There are two distinct limiting regimes of the irreversible colloidal aggregation process: the diffusion-limited CCA (DLCA) in dilute solutions and the reaction-limited CCA (RLCA) in dense solutions. The DLCA is due to the fast process determined by the time for the clusters to encounter each other by diffusion, and the RLCA is due to the slow process since the cluster-cluster repulsion has to dominate thermal activation.

Much of our understanding on the mechanism forming aggregates or flocs has been mainly due to computer simulations. The first simulation was carried out by Vold in 1963 [23], who used the ballistic aggregation model and found that the number of particles $N(r)$ within a distance r measured from the first seed particle is given by $N(r) \sim r^{2.3}$. Though this relation surely exhibits the scaling form of (2), the applicability of this model for real systems was doubted in later years. The researches on fractal aggregates has been developed from a simulation model on DLA introduced by T.A. Witten and L.M. Sander in 1981 [26] and on the DLCA model proposed by P. Meakin in 1983 [14] and M. Kolb et al. in 1983 [11], independently. The DLA has been used to describe diverse phenomena forming fractal patterns such as electro-depositions, surface corrosions and dielectric breakdowns. In the simplest version of the DLA model for irreversible colloidal aggregation, a particle is located at an initial site $\boldsymbol{r} = 0$ as a seed for cluster formation. Another particle starts a random walk from a randomly chosen site in the spherical shell of radius r with width $dr(\ll r)$ and center $\boldsymbol{r} = 0$. As a first step, a random walk is continued until the particle contacts the seed. The cluster composed of two particles is then formed. Note that the finite-size of particles is the very reason of dendrite structures of DLA. This procedure is repeated many times, in each of which the radius r of the starting spherical shell should be much larger than the gyration radius of the cluster. If the number of particles contained in the DLA cluster is huge (typically $10^4 \sim 10^8$), the cluster generated by this process is highly branched, and forms fractal structures in the meaning of statistical average. The fractality arises from the fact that the faster growing parts of the cluster shield the other parts, which there-

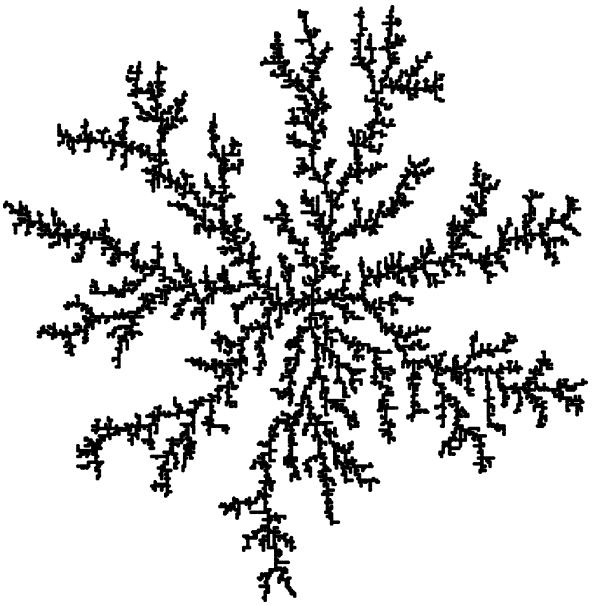

Fractal Structures in Condensed Matter Physics, Figure 5
Simulated results of a 2d diffusion-limited aggregation (DLA). The number of particles contained in this DLA cluster is 10^4

fore become less accessible to incoming particles. An arriving random walker is far more likely to attach to one of the tips of the cluster. Thus, the essence of the fractal-pattern formation arises surely from nonlinear process. Figure 5 illustrates a simulated result for a 2d DLA cluster obtained by the procedure mentioned above. The number of particles N inside a sphere of radius L ($\ll$ the gyration radius of the cluster) follows the scaling law given by

$$N \propto L^{D_f}, \tag{24}$$

where the fractal dimension takes a value of $D_f \approx 1.71$ for the 2d DLA cluster and $D_f \approx 2.5$ for the 3d DLA cluster without an underlying lattice. Note that these fractal dimensions are sensitive to the embedding lattice structure. The reason for this open structure is that a wandering molecule will settle preferentially near one of the tips of the fractal, rather than inside a cluster. Thus, different sites have different growth probabilities, which are high near the tips and decrease with increasing depth inside a cluster.

One of the most extensively studied DLA processes is the growth of metallic forms by electrochemical deposition. The scaling properties of electrodeposited metals were pointed out by R.M. Brady and R.C. Ball in 1984 for copper electrodepositions. The confirmation of the fractality for zinc metal leaves was made by M. Matsushita et al. in 1984. In their experiments [13], zinc metal leaves are grown two-dimensionally by electrodeposition. The structures clearly recover the pattern obtained by computer simulations for the DLA model proposed by T.A. Witten and L.M. Sander in 1981. Figure 6 shows a typical zinc

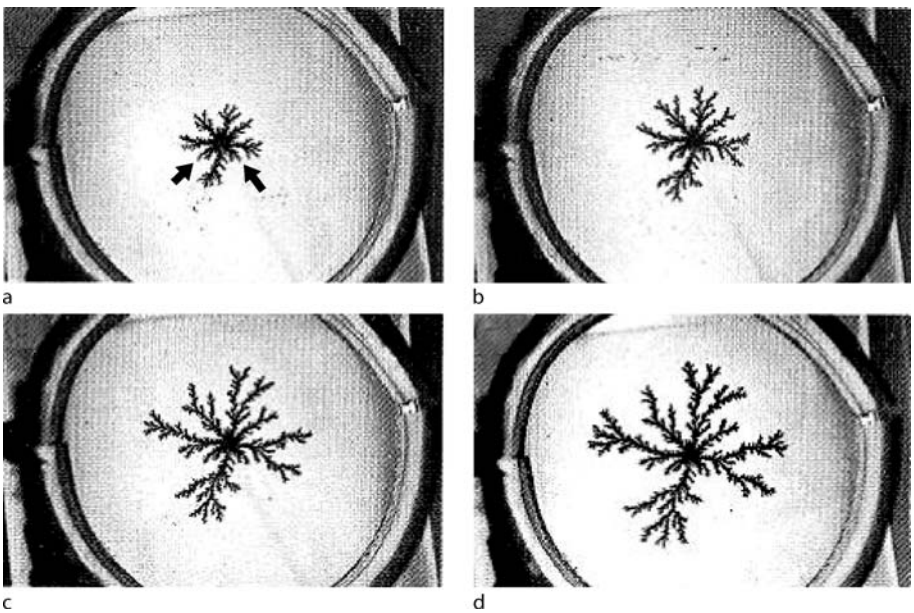

Fractal Structures in Condensed Matter Physics, Figure 6
The fractal structures of zinc metal leaves grown by electrodeposition. Photographs a–d were taken 3,5,9, and 15 min after initiating the electrolysis, respectively. After [13]

dendrite that was deposited on the cathode in one of these experiments. The fractal dimensionality $D_f = 1.66 \pm 0.33$ was obtained by computing the density-density correlation function $G(r)$ for patterns grown at applied voltages of less than 8V.

The fractality of uniformly sized gold-colloid aggregates according to the DLCA was experimentally demonstrated by D.A. Weitz in 1984 [25]. They used transmission-electron micrographs to determine the fractal dimension of this systems to be $D_f = 1.75$. They also performed quasi-elastic light-scattering experiments to investigate the dynamic characteristics of DLCA of aqueous gold colloids. They confirmed the scaling behaviors for the dependence of the mean cluster size on both time and initial concentration.

These works were performed *consciously* to examine the fractality of aggregates. There had been earlier works exhibiting the mass-size scaling relationship for actual aggregates. J.M. Beeckmans [2] pointed out in 1963 the power law behaviors by analyzing the data for aerosol and precipitated smokes in the literature (1922–1961). He used in his paper the term "aggregates-within-aggregates", implying the fractality of aggregates. However, the data available at that stage were not adequate and scattered. Therefore, this work did not provide decisive results on the fractal dimensions of aggregates. There were smarter experiments by N. Tambo and Y. Watanabe in 1967 [20], which precisely determined fractal dimensions of flocs formed in an aqueous solution. These were performed without being aware of the concept of fractals. Original works were published in Japanese. The English versions of these works were published in 1979 [21]. We discuss these works below.

Flocs generated in aqueous solutions have been the subject of numerous studies ranging from basic to applied sciences. In particular, the settling process of flocs formed in water incorporating kaolin colloids is relevant to water and wastewater treatment. The papers by N. Tambo and Y. Watanabe pioneered the discussion on the so-called *fractal approach* to floc structures; they performed their own settling experiments to clarifying the size dependences of mass densities for clay-aluminum flocs by using Stokes' law $u_r \propto \Delta\rho(r)r^2$ where $\Delta\rho$ is the difference between the densities of water and flocs taking so-small values $\Delta\rho \sim 0.01$–0.001 g/cm^3. Thus, the settling velocities u_r are very slow of the order of 0.001 m/sec for flocs of sizes $r \sim 0.1$ mm, which enabled them to perform precise measurements. Since flocs are very fragile aggregates, they made the settling experiments with special cautions on convection and turbulence, and by careful and intensive experiments of flocculation conditions. They confirmed from thousands of pieces of data the scaling relationship between settling velocities u_r and sizes of aggregates such as $u_r \propto r^b$. From the analysis of these data, they found the scaling relation between effective mass densities and sizes of flocs such as $\Delta\rho(r) \propto r^{-c}$, where the exponents c were found to take values from 1.25 to 1.00 depending on the aluminum-ion concentration, showing that the fractal dimensions become $D_f = 1.75$ to 2.00 with increasing aluminum-ion concentration. This is because the repulsive force between charged clay-particles is screened, and van der Waals attractive force dominates between the pair of particles. It is remarkable that these fractal dimensions D_f show excellent agreement with those determined for actual DLCA and RLCA clusters in the 1980s by using various experimental and computer simulation methods. Thus, they had found that the size dependences of mass densities of flocs are controlled by the aluminum-ion concentration dosed/suspended particle concentration, which they named the ALT ratio. These correspond

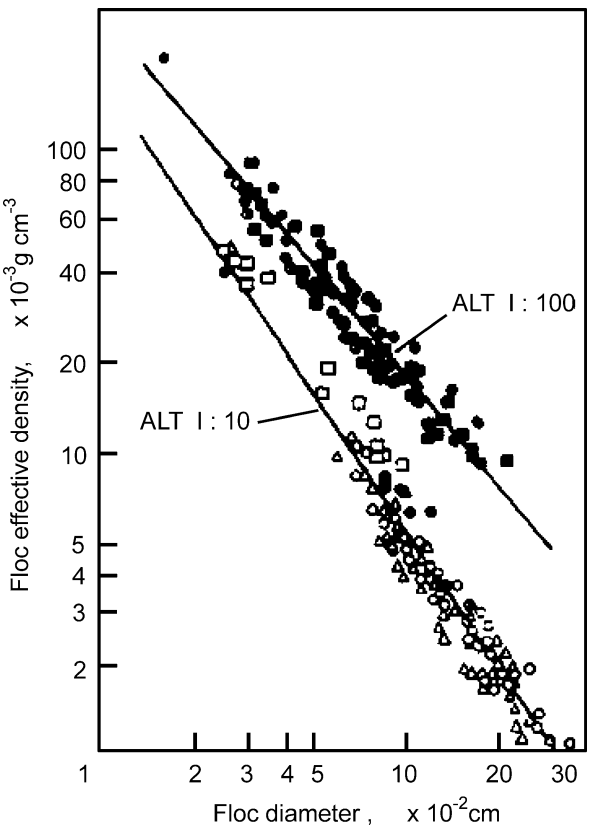

Fractal Structures in Condensed Matter Physics, Figure 7
Observed scaling relations between floc densities and their diameters where aluminum chloride is used as coagulants. After [21]

to the transition from DLCA (established now taking the value of $D_f \approx 1.78$ from computer simulations) process to the RLCA one (established at present from computer simulations as $D_f \approx 2.11$). The ALT ratio has since the publication of the paper been used in practice as a criterion for the coagulation to produce flocs with better settling properties and less sludge volume. We show their experimental data in Fig. 7, which demonstrate clearly that flocs (aggregates) are fractal.

Aerogels

Silica aerogels are extremely light materials with porosities as high as 98% and take fractal structures. The initial step in the preparation is the hydrolysis of an alkoxysilane $Si(OR)_4$, where R is CH_3 or C_2H_5. The hydrolysis produces silicon hydroxide $Si(OH)_4$ groups which polycondense into siloxane bonds –Si–O–Si–, and small particles start to grow in the solution. These particles bind to each other by *diffusion-limited cluster-cluster aggregation* (DLCA) (see Sect. "Aggregates and Flocs") until eventually they produce a disordered network filling the reaction volume. After suitable aging, if the solvent is extracted above the critical point, the open porous structure of the network is preserved and decimeter-size monolithic blocks with a range of densities from 50 to 500 kg/m^3 can be obtained. As a consequence, aerogels exhibit unusual physical properties, making them suitable for a number of practical applications, such as Cerenkov radiation detectors, supports for catalysis, or thermal insulators.

Silica aerogels possess two different length scales. One is the radius r of primary particles. The other length is the correlation length of the gel. At intermediate length scales, lying between these two length scales, the clusters possess a fractal structure and at larger length scales the gel is a homogeneous porous glass. Aerogels have a very low thermal conductivity, solid-like elasticity, and very large internal surfaces.

In elastic neutron scattering experiments, the scattering differential cross-section measures the Fourier components of spatial fluctuations in the mass density. For aerogels, the differential cross-section is the product of three factors, and is expressed by

$$\frac{d\sigma}{d\Omega} = Af^2(q)S(q)C(q) + B\,. \tag{25}$$

Here A is a coefficient proportional to the particle concentration and $f(q)$ is the primary-particle form factor. The structure factor $S(q)$ describes the correlation between particles in a cluster and $C(q)$ accounts for cluster-cluster correlations. The incoherent background is expressed by B. The structure factor $S(q)$ is proportional to the spatial Fourier transform of the density-density correlation function defined by (16), and is given by (17). Since the structure of the aerogel is fractal up to the correlation length ξ of the system and homogeneous for larger scales, the correlation function $G(r)$ is expressed by (25) for $r \ll \xi$ and $G(r) = \text{Const.}$ for $r \gg \xi$. Corresponding to this, the structure factor $S(q)$ is given by (17) for $q\xi \gg 1$, while $S(q)$ is independent of q for $q\xi \ll 1$. The wavenumber regime for which $S(q)$ becomes a constant is called the Guinier regime. The value of D_f can be deduced from the slope of the observed intensity versus momentum transfer ($q\xi \gg 1$) in a double logarithmic plot. For very large q, there exists a regime called the *Porod regime* in which the scattering intensity is proportional to q^{-4}.

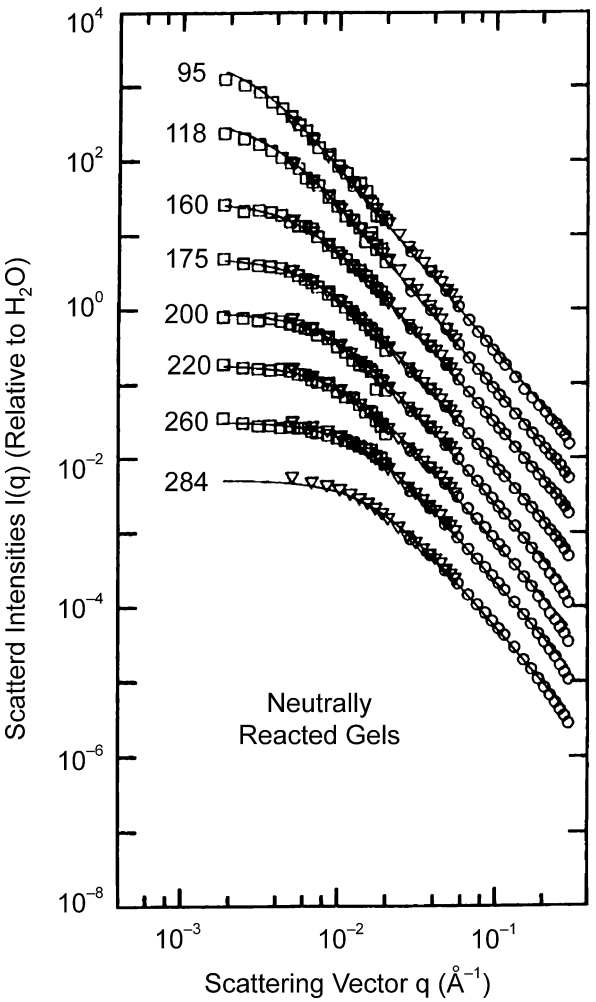

Fractal Structures in Condensed Matter Physics, Figure 8
Scattered intensities for eight neutrally reacted samples. Curves are labeled with ρ in kg/m^3. After [22]

The results in Fig. 8 by R. Vacher et al. [22] are from small-angle neutron scattering experiments on silica aerogels. The various curves are labeled by the macroscopic density ρ of the corresponding sample in Fig. 8. For example, 95 refers to a neutrally reacted sample with $\rho = 95\,\mathrm{kg/m^3}$. Solid lines represent best fits. They are presented even in the particle regime $q > 0.15\,\text{Å}^{-1}$ to emphasize that the fits do not apply in the region, particularly for the denser samples. Remarkably, D_f is independent of sample density to within experimental accuracy: $D_\mathrm{f} = 2.40 \pm 0.03$ for samples 95 to 360. The departure of $S(q)$ from the q^{-D_f} dependence at large q indicates the presence of particles with gyration radii of a few Å.

Dynamical Properties of Fractal Structures

The dynamics of fractal objects is deeply related to the time-scale problems such as diffusion, vibration and transport on fractal support. For the diffusion of a particle on any d-dimensional ordinary Euclidean space, it is well known that the mean-square displacement $\langle r^2(t)\rangle$ is proportional to the time such as $\langle r^2(t)\rangle \propto t$ for any Euclidean dimension d (see also (19)). This is called *normal diffusion*. While, on fractal supports, a particle more slowly diffuses, and the mean-square displacement follows the power law

$$\langle r^2(t)\rangle \propto t^{2/d_\mathrm{w}}\,, \tag{26}$$

where d_w is termed the exponent of *anomalous diffusion*. The exponents is expressed as $d_\mathrm{w} = 2 + \theta$ with a positive $\theta > 0$ (see (31)), implying that the diffusion becomes slower compared with the case of normal diffusion. This is because the inequality $2/d_\mathrm{w} < 1$ always holds. This slow diffusions on fractal supports are called *anomalous diffusion*.

The scaling relation between the length-scale and the time-scale can be easily extended to the problem of atomic vibrations of elastic fractal-networks. This is because various types of equations governing dynamics can be mapped onto the diffusion equation. This implies that both equations are governed by the same eigenvalue problem, namely, the replacement of eigenvalues $\omega \to \omega^2$ between the diffusion equation and the equation of atomic vibrations is justified. Thus, the basic properties of vibrations of fractal networks, such as the density of states, the dispersion relation and the localization/delocalization property, can be derived from the same arguments for diffusion on fractal networks. The dispersion relation between the frequency ω and the wavelength $\Lambda(\omega)$ is obtained from (26) by using the reciprocal relation $t \to \omega^{-2}$ (here the diffusion problem is mapped onto the vibrational one) and $\langle r^2(t)\rangle \to \Lambda(\omega)^{-2}$. Thus we obtain the dispersion relation for vibrational excitations on fractal networks such as

$$\omega \propto \Lambda(\omega)^{d_\mathrm{w}/2}\,. \tag{27}$$

If $d_\mathrm{w} = 2$, we have the ordinary dispersion relation $\omega \propto \Lambda(\omega)$ for elastic waves excited on homogeneous systems.

Consider the diffusion of a random walker on a *percolating fractal network*. How does $\langle r^2(t)\rangle$ behave in the case of fractal percolating networks? For this, P.G. de Gennes in 1976 [7] posed the problem called an ant in the labyrinth. Y. Gefen et al. in 1983 [9] gave a fundamental description of this problem in terms of a *scaling argument*. D. Ben-Avraham and S. Havlin in 1982 [3] investigated this problem in terms of Monte Carlo simulations. The work by Y. Gefen [9] triggered further developments in the dynamics of fractal systems, where the *spectral (or fracton)* dimension d_s is a key dimension for describing the dynamics of fractal networks, in addition to the fractal dimension D_f. The fractal dimension D_f characterizes how the geometrical distribution of a static structure depends on its length scale, whereas the spectral dimension d_s plays a central role in characterizing dynamic quantities on fractal networks. These dynamical properties are described in a unified way by introducing a new dynamic exponent called the *spectral or fracton* dimension defined by

$$d_\mathrm{s} = \frac{2D_\mathrm{f}}{d_\mathrm{w}}\,. \tag{28}$$

The term *fracton*, coined by S. Alexander and R. Orbach in 1982 [1], denotes vibrational modes peculiar to fractal structures. The characteristics of fracton modes cover a rich variety of physical implications. These modes are strongly localized in space and their localization length is of the order of their wavelengths.

We give below the explicit form of the exponent of anomalous diffusion d_w by illustrating percolation fractal networks. The mean-square displacement $\langle r^2(t)\rangle$ after a sufficiently long time t should follow the anomalous diffusion described by (26). For a finite network with a size ξ, the mean-square distance at sufficiently large time becomes $\langle r^2(t)\rangle \approx \xi^2$, so we have the diffusion coefficient for anomalous diffusion from (26) such as

$$D \propto \xi^{2-d_\mathrm{w}}\,. \tag{29}$$

For percolating networks, the diffusion constant D in the vicinity of the critical percolation density p_c behaves

$$D \propto (p - p_\mathrm{c})^{t-\beta} \propto \xi^{-(t-\beta)/\nu}\,, \tag{30}$$

where t is called the *conductivity exponent* defined by $\sigma_{dc} \sim (p - p_c)^t$, β the exponent for the percolation order parameter defined by $S(p) \propto (p - p_c)^\beta$, and ν the exponent for the correlation length defined by $\xi \propto |p - p_c|^{-\nu}$, respectively. Comparing (29) and (30), we have the relation between exponents such as

$$d_w = 2 + \frac{t - \beta}{\nu} = 2 + \theta \,. \tag{31}$$

Due to the condition $t > \beta$, and hence $\theta > 0$, implying that the diffusion becomes slow compared with the case of normal diffusion. This slow diffusion is called anomalous diffusion.

Spectral Density of States and Spectral Dimensions

The spectral density of states of atomic vibrations is the most fundamental quantity describing the dynamic properties of homogeneous or fractal systems such as specific heats, heat transport, scattering of waves and others. The simplest derivation of the spectral density of states (abbreviated, SDOS) of a homogeneous elastic system is given below. The density of states at ω is defined as the number of modes per particle, which is expressed by

$$D(\Delta\omega) = \frac{1}{\Delta\omega L^d} \,, \tag{32}$$

where $\Delta\omega$ is the frequency interval between adjacent eigenfrequencies close to ω and L is the linear size of the system. In the lowest frequency region, $\Delta\omega$ is the lowest eigenfrequency which depends on the size L. The relation between the frequency $\Delta\omega$ and L is obtained from the well-known linear dispersion relationship $\omega = \upsilon k$, where υ is the velocity of phonons (quantized elastic waves) such that

$$\Delta\omega = \frac{2\pi\upsilon}{\lambda} \propto \frac{1}{L} \,. \tag{33}$$

The substitution of (33) into (32) yields

$$D(\Delta\omega) \propto \Delta\omega^{d-1} \,. \tag{34}$$

Since this relation holds for any length scale L due to the scale-invariance property of homogeneous systems, we can replace the frequency $\Delta\omega$ by an arbitrary ω. Therefore, we obtain the conventional Debye density of states as

$$D(\omega) \propto \omega^{d-1} \,. \tag{35}$$

It should be noted that this derivation is based on the scale invariance of the system, suggesting that we can derive the SDOS for fractal networks in the same line with this treatment. Consider the SDOS of a fractal structure of size L with fractal dimension D_f. The density of states per particle at the lowest frequency $\Delta\omega$ for this system is, as in the case of (32), written as

$$D(\Delta\omega) \propto \frac{1}{L_f^D \Delta\omega} \,. \tag{36}$$

Assuming that the dispersion relation for $\Delta\omega$ corresponding to (33) is

$$\Delta\omega \propto L^{-z} \,, \tag{37}$$

we can eliminate L from (36) and obtain

$$D(\Delta\omega) \propto \Delta\omega^{D_f/z-1} \,. \tag{38}$$

The exponent z of the dispersion relation (37) is evaluated from the exponent of anomalous diffusion d_w. Considering the mapping correspondence between diffusion and atomic vibrations, we can replace $\langle r^2(t)\rangle$ and t by L^2 and $1/\Delta\omega^2$, respectively. Equation (26) can then be read as

$$L \propto \Delta\omega^{-2/d_w} \,. \tag{39}$$

The comparison of (28),(37) and (39) leads to

$$z = \frac{d_w}{2} = \frac{D_f}{d_s} \,. \tag{40}$$

Since the system has a scale-invariant fractal (self-similar) structure $\Delta\omega$, can be replaced by an arbitrary frequency ω. Hence, from (38) and (40) the SDOS for fractal networks is found to be

$$D(\omega) \propto \omega^{d_s-1} \,, \tag{41}$$

and the dispersion relation (39) becomes

$$\omega \propto L(\omega)^{-D_f/d_s} \,. \tag{42}$$

For percolating networks, the spectral dimension is obtained from (40)

$$d_s = \frac{2D_f}{2 + \theta} = \frac{2\upsilon D_f}{2\upsilon + \mu - \beta} \,. \tag{43}$$

This exponent d_s is called the *fracton dimension* after S. Alexander and R. Orbach [1] or the *spectral dimension* after R. Rammal and G. Toulouse [17], hereafter we use the term *spectral dimension* for d_s. S. Alexander and R. Orbach [1] estimated the values of d_s for percolating networks on d-dimensional Euclidean lattices from the known values of the exponents D_f, υ, μ and β. They

pointed out that, while these exponents depend largely on d, the spectral dimension (fracton) dimension d_s does not.

The spectral dimension d_s can be obtained from the value of the conductivity exponent t or vice versa. In the case of percolating networks, the conductivity exponent t is related to d_s through (43), which means that the conductivity $\sigma_{dc} \sim (p - p_c)^t$ is also characterized by the spectral dimension d_s. In this sense, the spectral dimension d_s is an intrinsic exponent related to the dynamics of fractal systems. We can determine the precise values of d_s from the numerical calculations of the spectral density of states of percolation fractal networks.

The fracton SDOS for 2d, 3d, and 4d bond percolation networks at the percolation threshold $p = p_c$ are given in Fig. 9a and b, which were calculated by K. Yakubo and T. Nakayama in 1989. These were obtained by large-scale computer simulations [27]. At $p = p_c$, the correlation length diverges as $\xi \propto |p - p_c|^{-\nu}$ and the network has a fractal structure at any length scale. Therefore, fracton SDOS should be recovered in the wide frequency range $\omega_L \ll \omega \ll \omega_D$, where ω_D is the Debye cutoff frequency and ω_L is the lower cutoff determined by the system size. The SDOSs and the integrated SDOSs per atom are shown by the filled squares for a 2d bond percolation (abbreviated, BP) network at $p_c = 0.5$. The lowest frequency ω_L is quite small ($\omega \sim 10^{-5}$ for the 2d systems) as seen from the results in Fig. 9 because of the large sizes of the systems. The spectral dimension d_s is obtained as $d_s = 1.33 \pm 0.11$ from Fig. 9a, whereas data in Fig. 9b give the more precise value $d_s = 1.325 \pm 0.002$. The SDOS and the integrated SDOS for 3d BP networks at $p_c = 0.249$ are given in Fig. 9a and b by the filled triangles (middle). The spectral dimension d_s is obtained as $d_s = 1.31 \pm 0.02$ from Fig. 9a and $d_s = 1.317 \pm 0.003$ from Fig. 9b. The SDOS and the integrated SDOS of 4d BP networks at $p_c = 0.160$.

A typical mode pattern of a fracton on a 2d percolation network is shown in Fig. 10a, where the eigenmode belongs to the angular frequency $\omega = 0.04997$. To bring out the details more clearly, Fig. 10b by K. Yakubo and T. Nakayama [28] shows cross-sections of this fracton mode along the line drawn in Fig. 10a. Filled and open circles represent occupied and vacant sites in the percolation network, respectively. We see that the fracton core (the largest amplitude) possesses very clear boundaries for the edges of the excitation, with an almost step-like character and a long tail in the direction of the weak segments. It should be noted that displacements of atoms in dead ends (weakly connected portions in the percolation network) move in phase, and fall off sharply at their edges.

The spectral dimension can be obtained exactly for deterministic fractals. In the case of the d-dimensional Sierpinski gasket, the spectral dimension is given by [17]

$$d_s = \frac{2\log(d+1)}{\log(d+3)} .$$

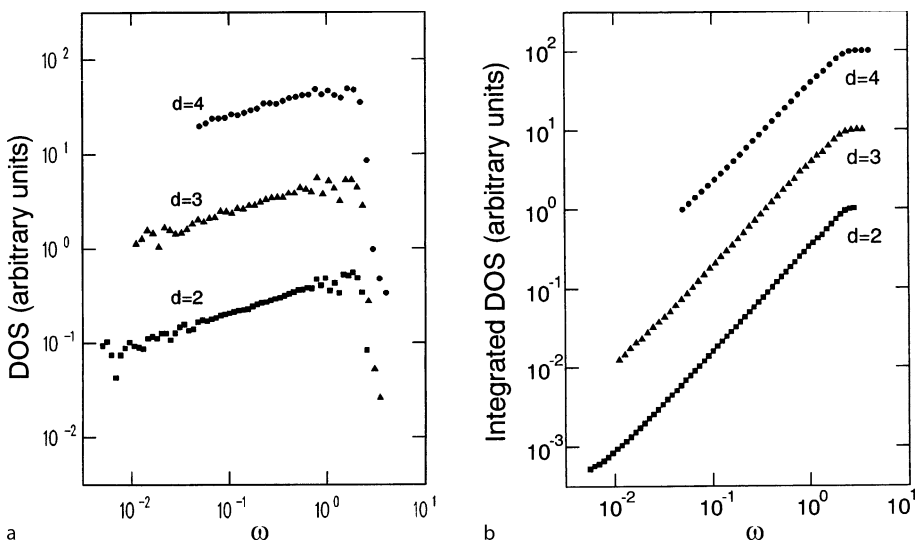

Fractal Structures in Condensed Matter Physics, Figure 9

a Spectral densities of states (SDOS) per atom for 2d, 3d, and 4d BP networks at $p = p_c$. The angular frequency ω is defined with mass units $m = 1$ and force constant $K_{ij} = 1$. The networks are formed on 1100 × 1100 (2d), 100 × 100 × 100 (3d), and 30 × 30 × 30 × 30 (4d) lattices with periodic boundary conditions, respectively. b Integrated densities of states for the same

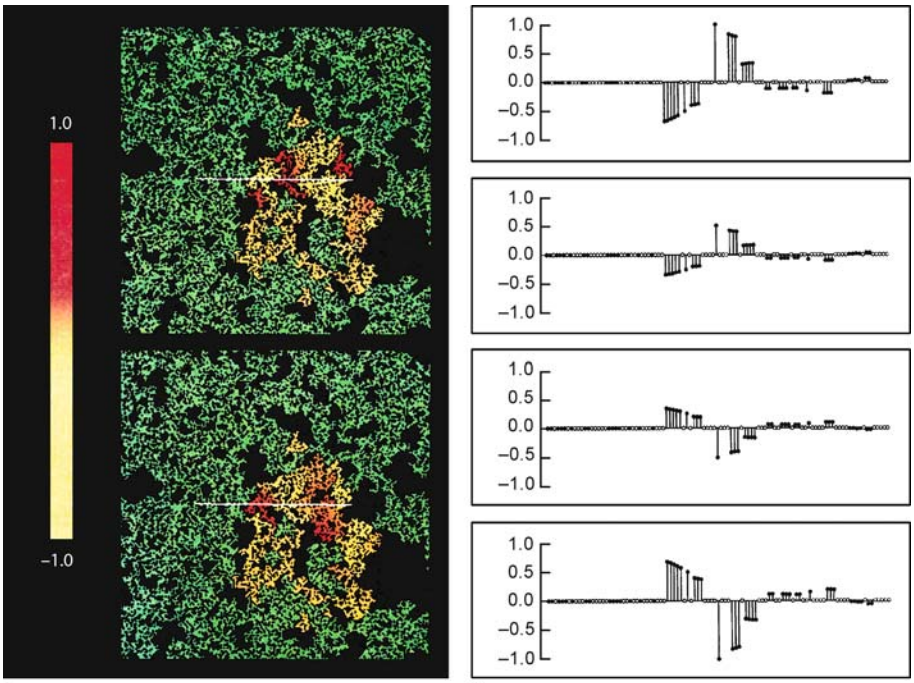

Fractal Structures in Condensed Matter Physics, Figure 10
a Typical fracton mode ($\omega = 0.04997$) on a 2d network. *Bright region* represents the large amplitude portion of the mode. b Cross-section of the fracton mode shown in a along the *white line*. The four figures are snapshots at different times. After [28]

We see from this that the upper bound for a Sierpinski gasket is $d_s = 2$ as $d \to \infty$. The spectral dimension for the Mandelbrot–Given fractal depicted is also calculated analytically as

$$d_s = \frac{2\log 8}{\log 22} = 1.345\ldots .$$

This value is close to those for percolating networks mentioned above, in addition to the fact that the fractal dimension $d_s = \log 8/\log 3$ of the Mandelbrot–Given fractal is close to $D_f = 91/48$ for 2d percolating networks and that the Mandelbrot–Given fractal has a structure with nodes, links, and blobs as in the case of percolating networks.

For real systems, E. Courtens et al. in 1988 [6] observed fracton excitations in aerogels by means of inelastic light scattering.

Future Directions

The significance of fractal researches in sciences is that the very idea of fractals opposes *reductionism*. Modern physics has developed by making efforts to elucidate the physical mechanisms of smaller and smaller structures such as molecules, atoms, and elementary particles. An example in condensed matter physics is the band theory of electrons in solids. Energy spectra of electrons can be obtained by incorporating group theory based on the translational and rotational symmetry of the systems. The use of this mathematical tool greatly simplifies the treatment of systems composed of 10^{22} atoms. If the energy spectrum of a unit cell *molecule* is solved, the whole energy spectrum of the solid can be computed by applying the group theory. In this context, the problem of an ordered solid is reduced to that of a unit cell. Weakly disordered systems can be handled by regarding impurities as a small perturbation to the corresponding ordered systems. However, a different approach is required for elucidating the physical properties of strongly disordered/complex systems with correlations, or of medium-scale objects, for which it is difficult to find an easily identifiable small parameter that would allow a perturbative analysis. For such systems, the concept of fractals plays an important role in building pictures of the realm of nature.

Our established knowledge on fractals is mainly due to experimental observations or computer simulations. The researches are at the phenomenological level stage, not at the intrinsic level, except for a few examples. Concerning future directions of the researches on fractals in condensed

matter physics apart from such a question as "What kinds of fractal structures are involved in condensed matter?", we should consider two directions: one is the very basic aspect such as the problem "Why are there numerous examples showing fractal structures in nature/condensed matter?" However, this type of question is hard. The kinetic growth-mechanisms of fractal systems have a rich variety of applications from the basic to applied sciences and attract much attention as one of the important subjects in non-equilibrium statistical physics and nonlinear physics. Network formation in society is one example where the kinetic growth is relevant. However, many aspects related to the mechanisms of network formations remain puzzling because arguments are at the phenomenological stage. If we compare with researches on Brownian motion as an example, the DLA researches need to advance to the stage of Einstein's intrinsic theory [8], or that of Smoluchowski [18] and H. Nyquist [15]. It is notable that the DLA is a stochastic version of the Hele–Shaw problem, the flow in composite fluids with high and low viscosities: the particles diffuse in the DLA, while the fluid pressure diffuses in Hele–Shaw flow [19]. These are deeply related to each other and involve *many open questions* for basic physics and mathematical physics.

Concerning the opposite direction, one of the important issues in fractal research is to explore practical uses of fractal structures. In fact, the characteristics of fractals are applied to many cases such as the formation of tailor-made nano-scale fractal structures, fractal-shaped antennae with much reduced sizes compared with those of ordinary antennae, and fractal molecules sensitive to frequencies in the infrared region of light.

Deep insights into fractal physics in condensed matter will open the door to new sciences and its application to technologies in the near future.

Bibliography

Primary Literature

1. Alexander S, Orbach R (1982) Density of states: Fractons. J Phys Lett 43:L625–631
2. Beeckmans JM (1963) The density of aggregated solid aerosol particles. Ann Occup Hyg 7:299–305
3. Ben-Avraham D, Havlin S (1982) Diffusion on percolation at criticality. J Phys A 15:L691–697
4. Brady RM, Ball RC (1984) Fractal growth of copper electro-deposits. Nature 309:225–229
5. Broadbent SR, Hammersley JM (1957) Percolation processes I: Crystals and mazes. Proc Cambridge Philos Soc 53:629–641
6. Courtens E, Vacher R, Pelous J, Woignier T (1988) Observation of fractons in silica aerogels. Europhys Lett 6:L691–697
7. de Gennes PG (1976) La percolation: un concept unificateur. Recherche 7:919–927
8. Einstein A (1905) Über die von der molekularkinetischen Theorie der Waerme geforderte Bewegung von in Ruhenden Fluessigkeiten Suspendierten Teilchen. Ann Phys 17:549–560
9. Gefen Y, Aharony A, Alexander S (1983) Anomalous diffusion on percolating clusters. Phys Rev Lett 50:70–73
10. Hausdorff F (1919) Dimension und Aeusseres Mass. Math Ann 79:157–179
11. Kolb M, Botel R, Jullien R (1983) Scaling of kinetically growing clusters. Phys Rev Lett 51:1123–1126
12. Mandelbrot BB, Given JA (1984) Physical properties of a new fractal model of percolation clusters. Phys Rev Lett 52: 1853–1856
13. Matsushita M, et al (1984) Fractal structures of zinc metal leaves grown by electro-deposition. Phys Rev Lett 53:286–289
14. Meakin P (1983) Formation of fractal clusters and networks by irreversible diffusion-limited aggregation. Phys Rev Lett 51:1119–1122
15. Nyquist H (1928) Termal agitation nof electric charge in conductors. Phys Rev 32:110–113
16. Perrin J (1909) Movement brownien et realite moleculaire. Ann Chim Phys 19:5–104
17. Rammal R, Toulouze G (1983) Random walks on fractal structures and percolation clusters. J Phys Lett 44:L13–L22
18. Smoluchowski MV (1906) Zur Kinematischen Theorie der Brownschen Molekular Bewegung und der Suspensionen. Ann Phys 21:756–780
19. Saffman PG, Taylor GI (1959) The penetration of a fluid into a porous medium or hele-shaw cell containing a more viscous fluid. Proc Roy Soc Lond Ser A 245:312–329
20. Tambo N, Watanabe Y (1967) Study on the density profiles of aluminium flocs I (in japanese). Suidou Kyoukai Zasshi 397:2–10; ibid (1968) Study on the density profiles of aluminium flocs II (in japanese) 410:14–17
21. Tambo N, Watanabe Y (1979) Physical characteristics of flocs I: The floc density function and aluminium floc. Water Res 13:409–419
22. Vacher R, Woignier T, Pelous J, Courtens E (1988) Structure and self-similarity of silica aerogels. Phys Rev B 37:6500–6503
23. Vold MJ (1963) Computer simulation of floc formation in a colloidal suspension. J Colloid Sci 18:684–695
24. Weitz DA, Oliveria M (1984) Fractal structures formed by kinetic aggregation of aqueous cold colloids. Phys Rev Lett 52: 1433–1436
25. Weitz DA, Huang JS, Lin MY, Sung J (1984) Dynamics of diffusion-limited kinetics aggregation. Phys Rev Lett 53:1657–1660
26. Witten TA, Sander LM (1981) Diffusion-limited aggregation, a kinetic critical phenomenon. Phys Rev Lett 47:1400–1403
27. Yakubo K, Nakayama T (1989) Direct observation of localized fractons excited on percolating nets. J Phys Soc Jpn 58: 1504–1507
28. Yakubo K, Nakayama T (1989) Fracton dynamics of percolating elastic networks: energy spectrum and localized nature. Phys Rev B 40:517–523

Books and Reviews

Barabasi AL, Stanley HE (1995) Fractal concepts in surface growth. Cambridge University Press, Cambridge

Ben-Avraham D, Havlin S (2000) Diffusion and reactions in fractals and disordered systems. Cambridge University Press, Cambridge

Bunde A, Havlin S (1996) Fractals and disordered systems. Springer, New York
de Gennes PG (1979) Scaling concepts in polymer physics. Cornell University Press, Itahca
Falconer KJ (1989) Fractal geometry: Mathematical foundations and applications. Wiley, New York
Feder J (1988) Fractals. Plenum, New York
Flory PJ (1969) Statistical mechanics of chain molecules. Inter Science, New York
Halsey TC (2000) Diffusion-limited aggregation: A model for pattern formation. Phys Today 11:36–41
Kadanoff LP (1976) Domb C, Green MS (eds) Phase transitions and critical phenomena 5A. Academic Press, New York
Kirkpatrick S (1973) Percolation and conduction. Rev Mod Phys 45:574–588
Mandelbrot BB (1979) Fractals: Form, chance and dimension. Freeman, San Francisco
Mandelbrot BB (1982) The fractal geometry of nature. Freeman, San Francisco
Meakin P (1988) Fractal aggregates. Adv Colloid Interface Sci 28:249–331
Meakin P (1998) Fractals, scaling and growth far from equilibrium. Cambridge University Press, Cambridge
Nakayama T, Yakubo K, Orbach R (1994) Dynamical properties of fractal networks: Scaling, numerical simulations, and physical realizations. Rev Mod Phys 66:381–443
Nakayama T, Yakubo K (2003) Fractal concepts in condensed matter. Springer, Heidelberg
Sahimi M (1994) Applications of percolation theory. Taylor and Francis, London
Schroeder M (1991) Fractals, chaos, power laws. W.H. Freeman, New York
Stauffer D, Aharony A (1992) Introduction to percolation theory, 2nd edn. Taylor and Francis, London
Vicsek T (1992) Fractal growth phenomena, 2nd edn. World Scientific, Singapore

Fractals and Wavelets: What Can We Learn on Transcription and Replication from Wavelet-Based Multifractal Analysis of DNA Sequences?

Alain Arneodo[1], Benjamin Audit[1], Edward-Benedict Brodie of Brodie[1], Samuel Nicolay[2], Marie Touchon[3,5], Yves d'Aubenton-Carafa[4], Maxime Huvet[4], Claude Thermes[4]

[1] Laboratoire Joliot–Curie and Laboratoire de Physique, ENS-Lyon CNRS, Lyon Cedex, France
[2] Institut de Mathématique, Université de Liège, Liège, Belgium
[3] Génétique des Génomes Bactériens, Institut Pasteur, CNRS, Paris, France
[4] Centre de Génétique Moléculaire, CNRS, Gif-sur-Yvette, France
[5] Atelier de Bioinformatique, Université Pierre et Marie Curie, Paris, France

Article Outline

Glossary
Definition of the Subject
Introduction
A Wavelet-Based Multifractal Formalism: The Wavelet Transform Modulus Maxima Method
Bifractality of Human DNA Strand-Asymmetry Profiles Results from Transcription
From the Detection of Relication Origins Using the Wavelet Transform Microscope to the Modeling of Replication in Mammalian Genomes
A Wavelet-Based Methodology to Disentangle Transcription- and Replication-Associated Strand Asymmetries Reveals a Remarkable Gene Organization in the Human Genome
Future Directions
Acknowledgments
Bibliography

Glossary

Fractal Fractals are complex mathematical objects that are invariant with respect to dilations (**self-similarity**) and therefore do not possess a characteristic length scale. Fractal objects display scale-invariance properties that can either fluctuate from point to point (**multifractal**) or be homogeneous (**monofractal**). Mathematically, these properties should hold over all scales. However, in the real world, there are necessarily lower and upper bounds over which self-similarity applies.

Wavelet transform The continuous wavelet transform (WT) is a mathematical technique introduced in the early 1980s to perform time-frequency analysis. The WT has been early recognized as a mathematical microscope that is well adapted to characterize the scale-invariance properties of fractal objects and to reveal the hierarchy that governs the spatial distribution of the singularities of multifractal measures and functions. More specifically, the WT is a space-scale analysis which consists in expanding signals in terms of wavelets that are constructed from a single function, the analyzing wavelet, by means of translations and dilations.